REGIONAL MAGNITUDE RESEARCH SUPPORTING BROAD-AREA MONITORING OF SMALL SEISMIC EVENTS

W. Scott Phillips, Howard J. Patton, Richard J. Stead, George E. Randall, and Hans E. Hartse

Los Alamos National Laboratory

Sponsored by National Nuclear Security Administration
Office of Nonproliferation Research and Development
Office of Defense Nuclear Nonproliferation

Contract No. DE-AC52-06NA25396

ABSTRACT

The Los Alamos National Laboratory's Ground-Based Nuclear Explosion Monitoring Research and Engineering (GNEMRE) Program has a long-standing magnitude research project in support of regional yield estimation and source discrimination. This project has developed magnitude-yield scaling relationships based on regional P, S phases and coda waves to improve our capabilities to monitor nuclear explosions over broad areas and at low yields. Due to the great variability of regional seismograms, the methods developed for broad-area monitoring must be adaptable to different phases and frequency bands. These requirements, along with an understanding of the transportability of scaling relationships, pose a significant challenge from both practical and theoretical standpoints since any broad-area method needs a sound physical basis to be ultimately successful.

Coda wave efforts have recently focused on practical aspects such as schema design for the exchange of calibration parameters and details of signal processing coding to match measurements between institutions, as well as advanced aspects of extending near-regional coda techniques to broad area and far-regional distances. We have developed the MagYield 0.10 schema, which ties to National Nuclear Security Administration (NNSA) Knowledge Base (KB) core schema for the exchange of envelope recipes, coda calibration parameters, and yield regression parameters. Exacting tests of signal processing methods between institutions uncovered issues with a widely used deconvolution code and code-dependent effects of non-ideal bandwidth/Nyquist ratios. Extension of the coda method to broad area far-regional distances showed the importance of 2-D path effects, as well as 2-D phase type (P vs. Sn vs. Lg coda) and 2-D transfer function effects. A detailed investigation of a near- regional data set from the Korean Peninsula showed that large numbers of small, low stress events can cause bias in the empirical Green's function (EGF) phase of coda calibration, leading to slight spectral peaking near 1 Hz and coda moments that do not scale one-to-one with independent estimates. This is mitigated by weighting EGF data by low frequency spectral slope, leading to an automatic method that can be applied uniformly to different regions.

We continue to study multi-frequency relative scaling observations of Pn and Lg-coda waves for explosions detonated at the Nevada Test Site (NTS) and the Semipalatinsk Test Site (STS). Observations for both test sites show that Pn amplitudes yield scale 10-30% higher than coda amplitudes for high frequencies between 2-8 Hz. The contrast in scaling shows strong frequency dependence at NTS for lower frequencies, with Pn scaling as much as 50% higher than Lg coda waves for frequencies near 0.6 Hz. On the other hand, Pn and coda amplitudes for STS explosions do not scale differently for any frequency band less than 2 Hz. These observations have implications for yield estimation and seismic discrimination, among them being that high-frequency phase ratios should display yield dependence. We have developed a model that predicts the observed scaling differences at high frequencies. Two essential elements of the model are (1) Rg generation by a compensated linear vector dipole (CLVD) and (2) near-source scattering of Rg as the source of S waves making up Lg and Lg coda. The CLVD is a kinematic representation for tensile failure related to non-linear interactions of explosion shock waves with the free surface. Work on this model continues with the goal to explain the strong frequency dependence of NTS observations and the reason(s) for differences in relative scaling between NTS and STS.

OBJECTIVES

We seek to improve yield estimation and seismic discrimination capabilities for broad areas and small events through the development of regional magnitude methodologies and data sets of direct phases and coda waves. Our research advances the state of the art in nuclear monitoring though (1) characterization of the scaling behavior and transportability of regional magnitudes based on path-corrected amplitudes using advanced calibration techniques and (2) development of physical models to interpret the observations and to lay a physical basis supporting operational techniques.

RESEARCH ACCOMPLISHED

Broad area coda calibration. We calibrate coda amplitudes for purposes of determining Mw, which is used in event identification procedures, and yield, via direct comparison to test site results for high frequencies (>1 Hz). Coda techniques are known to be effective over near-regional distances (Mayeda et al., 2003), and for comparing events in the same source region at far regional distances. Our challenge is to extend the coda technique to broad areas and far regional distances over our central and eastern Asia study region (Figure 1). This requires two-dimensional (2-D) calibration. Phillips et al. (2001) have demonstrated the effectiveness of 2-D path calibration. 2-D calibration is especially critical for events for which both continental and oceanic paths are observed, due to varying levels of blockage of the Lg, and Lg coda, and we have begun to include oceanic paths in our data set to investigate techniques to account for this.

Full 2-D, broad area calibration begins with differentiating between various coda types. Figure 2 shows group velocities of the beginning of the coda, which often, but not always, correspond to the envelope peak, for three frequency bands. We observe Lg, Sn and P coda over regional distances, with Lg dominant at short distances and lower bands. Figure 3 shows the distribution of coda types for station WMQ in western China and also indicates 2-D variations within the Lg type. We see that Sn coda are observed at shorter distances across regions of low crustal Q, such as Tibet. Thus, both coda type and the group velocity variations within a given type vary laterally and this must be accounted for using station centric lookup tables or tomographic models. Strategies for doing so remain to be tested.

We use a spectral EGF technique to extend absolute measures of spectra, based on ground truth moments, to the higher bands (> 1 Hz) that are important for yield estimation. Thus, the calculation of the transfer function terms, via EGF, is a critical calibration step. We solve for the frequency dependent transfer terms by requiring spectra from a large group of events to fit a Brune model for bands well below individual estimates of corner frequency. Corner frequency is estimated crudely based on magnitude (e.g., Walter and Taylor, 2001). Effects of the crude estimate are mitigated by limiting to a factor of 4 below the corner. In a focused study of events from the Korean Peninsula, we found that low frequency spectral slopes are not flat, in a relative sense, but can vary by a few tenths from event to event, with some dependence on source region. This may be due to regional variation in apparent stress. Without investigating the root cause further, we weighted the higher slope (higher stress) events more heavily in the EGF procedures and obtained more realistic spectra (slight spectral peaks at 1 Hz disappeared), and ground truth moments scaled one-to-one with coda moments (a slight deviation for small events due to the aforementioned 1 Hz peaks disappeared).

Furthermore, we developed a 2-D, EGF technique to account for variation of the transfer function across our study region. Results show a regional variation (Figure 4) that primarily reflects differences in the dominant coda types. This variation is best accounted for at an earlier stage of calibration by splitting into Lg and Sn coda, applying corrections for different path effects and a differential transfer term before combining results together. Tests of such methods remain to be performed and rely on data sets from low Q crustal regions to estimate Sn coda path effects at the shortest possible distances. Results of comparing ground truth and coda moments after applying the 2-D transfer function shows good agreement, especially for continental events evaluated using regional techniques (Figure 5).

Observations of Pn, Lg-Coda scaling differences. We continue to study multi-frequency relative scaling observations of Pn and Lg-coda waves for explosions detonated at the NTS and the STS. Relative scaling slopes

were estimated using two methods. Briefly, the first method determines the relative scaling slope (Pn relative to Lg coda) from regressions on log-log plots of coda versus Pn amplitudes, passed through identical narrow-band filters (see Patton and Phillips, 2005). If the explosions are located in small enough test area, the path effects to a given station should be the same. The second method utilizes ground-truth yields to perform separate amplitude-yield regressions on Pn and coda amplitudes; relative scaling slopes were obtained by taking the ratio of the estimated yield slopes. In carrying out the yield regressions, the effect of gas porosity was accounted for. All amplitudes were subjected to signal-to-noise (SNR) checks: SNR for Lg-coda waves decrease rapidly above ~6 Hz for Livermore NTS Network recordings. Nevertheless, it is clear that the codas are those of Lg waves for all bands, as *Sn* is not as well recorded on this network compared to Lg. On the other hand, Lg amplitudes recorded at Borovoye for STS explosions can drop below the level of Sn-coda waves for frequency bands above the 2–3 Hz passband. Thus, even though many recordings of the Borovoye archive (Kim et al., 2001) are well above the noise levels at high frequencies, our measurement windows contain a superposition of Sn and Lg codas.

Figure 6 is a summary of scaling results for NTS explosions. Narrow frequency passbands used for filtering the amplitudes are denoted with horizontal lines on the abscissa. The results for both methods are in reasonably good agreement for stations Elko (ELK) and Kanab (KNB). Both stations have similar frequency dependence, showing rapid change at low frequencies, going from no scaling differences in the lowest band to 50%–60% faster scaling for Pn relative to Lg coda in the next band, 0.5–0.7 Hz. With the exception of the lowest band, the results of all bands indicate that Pn amplitudes scale at a higher rate than Lg coda amplitudes, and the close agreement between results of both methods strengthen the reliability of these findings. Plotted with the observations is the prediction based on the Fisk conjecture (Fisk, 2006; 2007) using NTS parameters specified in Figure 3 of Mueller and Murphy (1971). P and S slopes used for the model calculations are means for a yield range between 0.1 and 1000 kt. An important question to answer is why are there significant departures in the observations at low and high frequencies from the prediction, which is based on the Mueller-Murphy model and on differences in the P and S corner frequencies according to the Fisk conjecture.

Near-source scattering mechanisms for S wave generation. A key tenet of near-source scattering mechanisms proposed for regional phase generation is that the amplitude-frequency dependence of the input wave should be imprinted onto the scattered waves. This tenet traces its roots to early studies using coda waves to extract source spectra (e.g., Aki, 1969), and can be justified if the scattering transfer function is linear and varies smoothly across the frequency band of interest. In the case of near-field scattering of P waves into S, the P-wave source spectrum is imprinted on the scattered S waves (e.g., P-wave imprinting). Gupta et al. (1992) were the first to suggest that near-source scattering of Rg waves makes a significant contribution to low-frequency (< 2 Hz) Lg. Under this hypothesis, the frequency dependence of Rg amplitudes is imprinted onto subsequently scattered P and S waves and is called Rg imprinting.

The first studies to support Rg imprinting used spectra of Lg waves for Yucca Flats, NTS, and Semipalatinsk explosions (Patton and Taylor, 1995, referred to as PT95; Gupta et al., 1997). PT95 studied spectral ratios for nearby Yucca Flats shots, one at normal containment depth (normal buried, NB) and the other an overburied (OB) shot serving as an empirical Green's function. A prominent null was observed in the spectral ratios near 0.55 Hz. According to PT95, an explosion is comprised of an initial burst, represented by a monopole force system, plus a source of tensile failure, represented by a compensated linear vector dipole (CLVD). In their model, the CLVD excites Rg waves much stronger than the monopole does for NB explosions, and the spectral null is caused by an effect of CLVD source depth on Rg excitation and is imprinted onto the scattered S waves making up Lg.

Recent modeling work has revealed that a CLVD source as strong as that proposed by PT95 violates long-period Rayleigh wave phase observations (Patton and Phillips, 2006). A new source model was developed to fit Lg spectral ratios without violating the long periods and over a broader frequency range than PT95 modeled. The interested reader is referred to Patton and Phillips for details about the new model. Even though the model uses simple analytic solutions for a half-space medium and is still under development, it makes two very interesting predictions: (1) at low frequencies (< ~2Hz), the ratios should be characterized by spectral modulations resulting from interference of Rg waves emitted by the CLVD and monopole sources and (2) at high frequencies, the Rg excitation is dominated by the CLVD. The first prediction is consistent with the general characteristics of Lg spectral ratios for NTS explosions, while the second has interesting implications for observed yield scaling differences between P and Lg.

Before discussing the effects on regional phase scaling observations, we briefly summarize the evidence for Rg imprinting utilizing a new integrative analysis approach involving difference spectrograms (Gupta et al., 2007).

Difference spectrograms. A spectrogram may be considered a two-dimensional matrix of numbers providing amplitude and frequency information for each point of a time series. The new method of Gupta et al. takes the point-by-point difference of log amplitudes between spectrograms of two nearby explosions recorded at a common station. As with the spectral ratio approach, if one of the explosions is overburied, the source characteristics of the NB explosion can be isolated in the resultant difference spectrogram since the OB shot acts as an empirical Green's function.

Figure 7a, taken from Gupta et al. (2007), shows the difference spectrogram of Rousanne (NB) and Techado (OB) on Yucca Flats for station ELK. The difference spectrogram was obtained by (1) aligning the Pn onsets, (2) obtaining noise-corrected log amplitude spectrograms using a moving time window of 12.8 s with a time shift of 0.5 s, (3) subtracting three-dimensional matrices of log amplitudes (Rousanne-Techado), and (4) contour plotting the resulting values after converting to linear amplitude and smoothing. Amplitude modulations can be seen on the difference spectrogram with spectral nulls at ~0.55 Hz and 1.1 Hz. The null at 0.55 Hz seems to start in the Pg coda and is expressed at several different times within the Lg wavetrain and coda.

Figures 7b–d show spectral ratios for time windows corresponding to Pg coda, Lg, and Lg coda. The ELK results in all three windows are good general agreement with the results for the four-station Livermore-network average. Vertical dash lines correspond to the frequencies where the spectrogram shows persistent nulls. The null at 0.55 Hz is most clearly expressed for Lg coda and is weakly expressed for Pg coda. Figure 7e shows a summary of spectral ratios for Pg coda, Lg, and Lg coda plus for a window corresponding to the arrival of Pn and its coda. Note that the Pn spectral ratio shows no evidence of modulation for frequencies below 1 Hz, consistent with the difference spectrogram. Gupta et al. interpret amplitude modulations at low frequencies (< ~2 Hz) observed for Pg coda, Lg, and Lg coda as a consequence of Rg imprinting.

Rg imprinting and implications for regional phase scaling. It has not escaped our attention that the most serious discrepancy between the Fisk prediction and the relative scaling observations presented above corresponds to the frequency band 0.5–0.7 Hz, where a strong amplitude null exists in the spectral ratios and difference spectrograms for Lg and Lg coda, but not for Pn waves. Furthermore, the high frequency discrepancies in Figure 6 occur in the frequency range where the model of Patton and Phillips predicts that the CLVD should be controlling the excitation of Rg waves. Patton and Phillips (2006) provide a "back-of-the-envelope" calculation assuming some scaling relationships for the CLVD source. This calculation supports the notion that Rg waves might yield scale at a lower rate than P waves for the Mueller-Murphy model at high frequencies, consistent with the observations for Pn and Lg coda waves. Hence, Rg imprinting could be the cause of scaling differences between Pn waves and regional shear phases, like Lg and its coda.

CONCLUSIONS AND RECOMMENDATIONS

In order to calibrate coda amplitudes over broad areas and to far regional distances we must work to extend 2-D coda calibration to coda type, shape, and transfer function steps, accounting for superposed Lg and Sn coda. This requires analysis of data from regions of low crustal Q in order to measure Sn coda over the widest range of distances. Further, interest in monitoring source regions near coastlines requires similar efforts to account for partial and full blockage of Lg and Lg coda over oceanic paths.

Because of the potential importance of near-field scattering in the generation of regional phases by underground explosions, we are starting the groundwork on a new scaling model for asymmetric explosion sources involving the superposition of monopole and CLVD force systems. This model will be applied to the problem of Rg excitation to investigate whether or not variations in Rg scaling with respect to Mueller-Murphy scaling for P can mimic the relative scaling observations in Figure 6 across the entire frequency range. There is much work to be done to develop a CLVD source model and associated scaling relationships.

ACKNOWLEDGEMENTS

We thank the LANL GNEMRE team for bulletin integration, event location, waveform acquisition, and database support.

REFERENCES

Aki, K. (1969). Analysis of the seismic coda of local earthquakes as scattered waves, *J. Geophys. Res.* 74: 615–631.

Fisk, M. D. (2006). Source spectral modeling of regional P/S discriminants at nuclear test sites in China and the former Soviet Union, *Bull. Seismol. Soc. Am.* 96: 2348–2367.

Fisk, M. D. (2007). Corner frequency scaling of regional seismic phases for underground nuclear explosions at the Nevada Test Site, *Bull. Seismol. Soc. Am.* 97: 977–988.

Gupta, I. N., W. Chan, and R. Wagner (1992). A comparison of regional phases from underground nuclear explosions at East Kazakh and Nevada Test Sites, *Bull. Seismol. Soc. Am.* 82: 352–382.

Gupta, I. N., T. Zhang, and R. Wagner (1997). Low-frequency Lg from NTS and Kazakh nuclear explosions—Observations and interpretation, *Bull. Seismol. Soc. Am.* 87: 1115-1125.

Gupta, I. N., H. J. Patton, W. W. Chan, H. A. A. Ghalib, and R. A. Wagner (2007). Difference spectrograms: A new method for studying S-wave generation from explosions, *Bull. Seismol. Soc. Am.* (submitted).

Kim, W.-Y., P. G. Richards, V. Adushkin, and V. Ovtchinnikov (2001). Borovoye digital archive for underground nuclear tests during 1966–1996, Data report on the web at http://www.ldeo.columbia.edu/res/pi/Monitoring/Data/brv_exp_archive.html, Borovoye Archive for UNT (information product in PDF).

Mayeda, K., A. Hofstetter, J. L. O'Boyle, and W. R. Walter (2003). Stable and transportable regional magnitudes based on coda-derived moment-rate spectra, *Bull. Seism. Soc. Am.* 93: 224–239.

Mueller, R. A. and J. R. Murphy (1971). Seismic characteristics of underground nuclear detonations, Part I: Seismic spectrum scaling, *Bull. Seismol. Soc. Am.* 61: 1675–1692.

Patton, H. J. and S. R. Taylor (1995). Analysis of Lg spectral ratios from NTS explosions: Implications for the source mechanisms of spall and the generation of Lg waves, *Bull. Seismol. Soc. Am.* 85: 220–236.

Patton, H. J. and W. S. Phillips (2005). Regional magnitude research supporting broad-area monitoring of small seismic events, in *Proceedings of the 27th Seismic Research Review: Ground-Based Nuclear Explosion Monitoring Technologies*, LA-UR-05-6407, Vol. I, pp. 606–611.

Patton, H. J. and W. S. Phillips (2006). Regional magnitude research supporting broad-area monitoring of small seismic events, in *Proceedings of the 28th Seismic Research Review: Ground-Based Nuclear Explosion Monitoring Technologies*, LA-UR-06-5471, Vol. 1, pp. 646–653.

Phillips, W. S., H. J. Patton, H. E. Hartse, and K. M. Mayeda (2001). Regional coda magnitudes in Central Asia and mb(Lg) transportability, in *Proceedings of the 23rd Seismic Research Review: Worldwide Monitoring of Nuclear Explosions*, LA-UR-01-4454, Vol.1, pp. 580–589.

Walter, W. R and S. R. Taylor (2001). A revised magnitude and distance amplitude correction (MDAC2) procedure for regional seismic discriminants: Theory and testing at NTS, Lawrence Livermore National Laboratory report UCRL-ID-146882, http://www.llnl.gov/tid/lof/documents/pdf/240563.pdf.

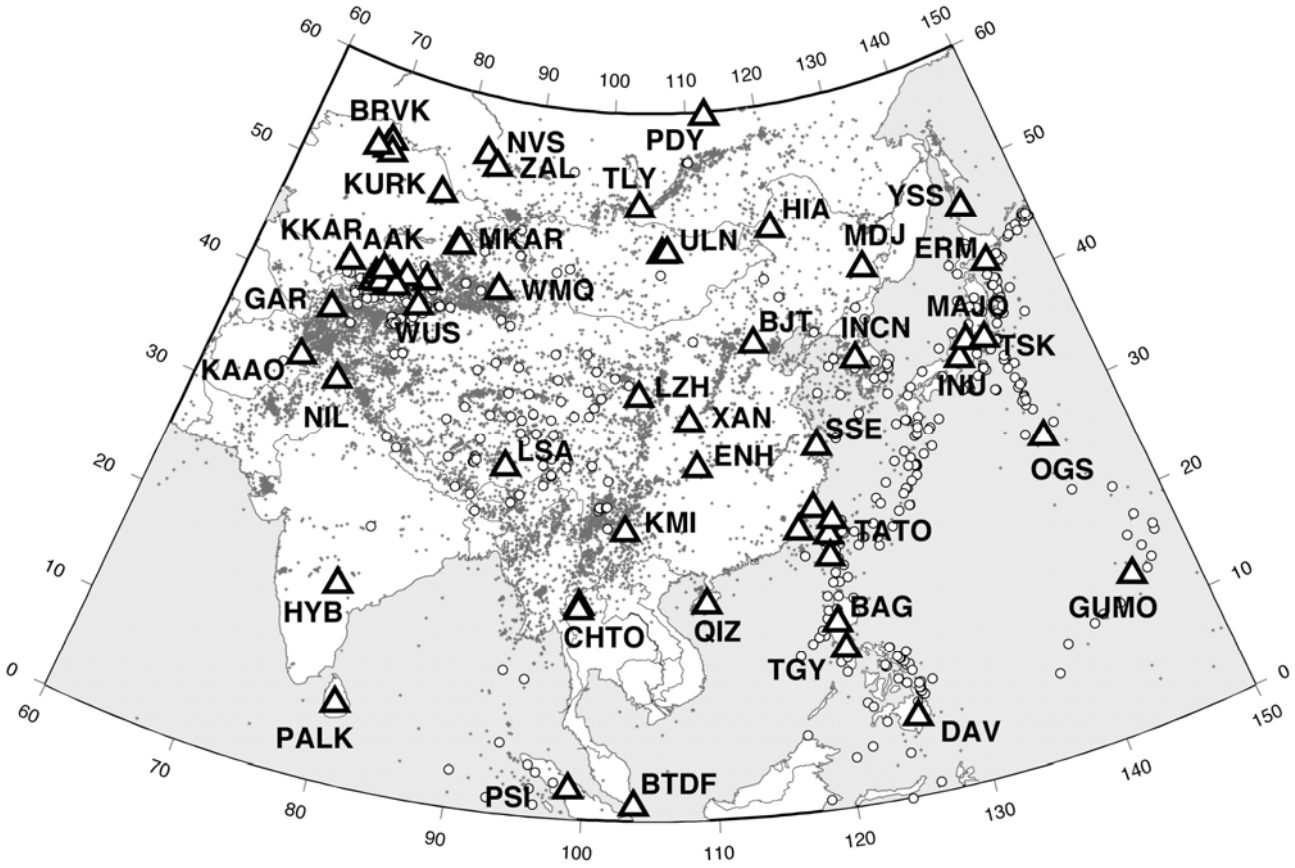

Figure 1. Stations (triangles) and events (dots) used in the broad area coda study. Open circles indicate ground truth moment events.

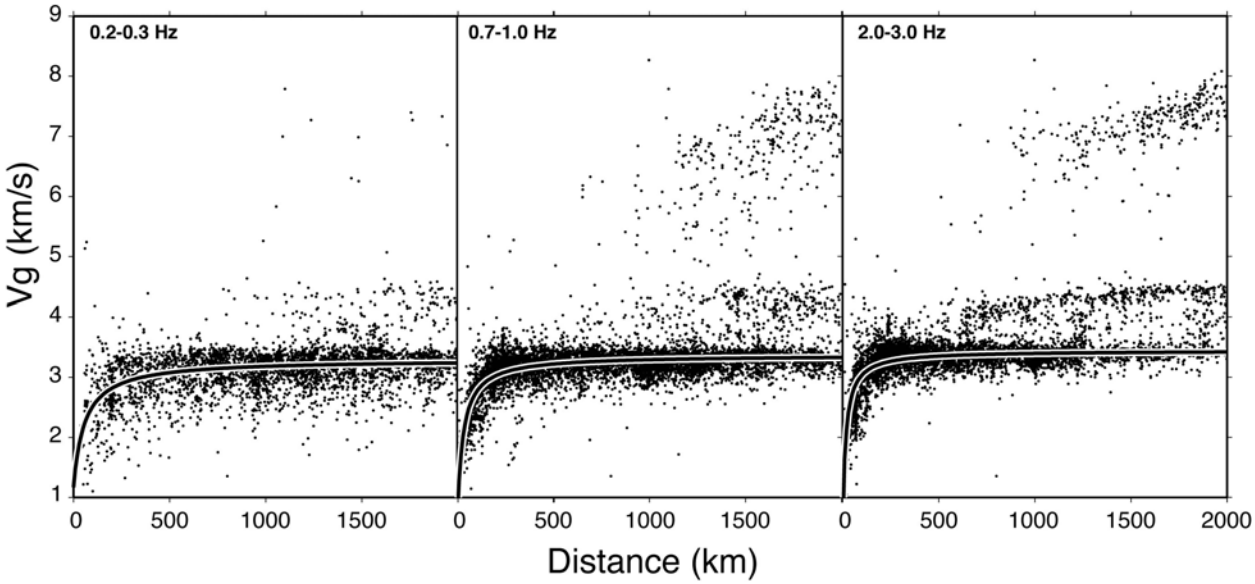

Figure 2. Group velocity of the beginning of the coda (manually picked) versus distance for three bands. The fitted curve represents the Lg branch.

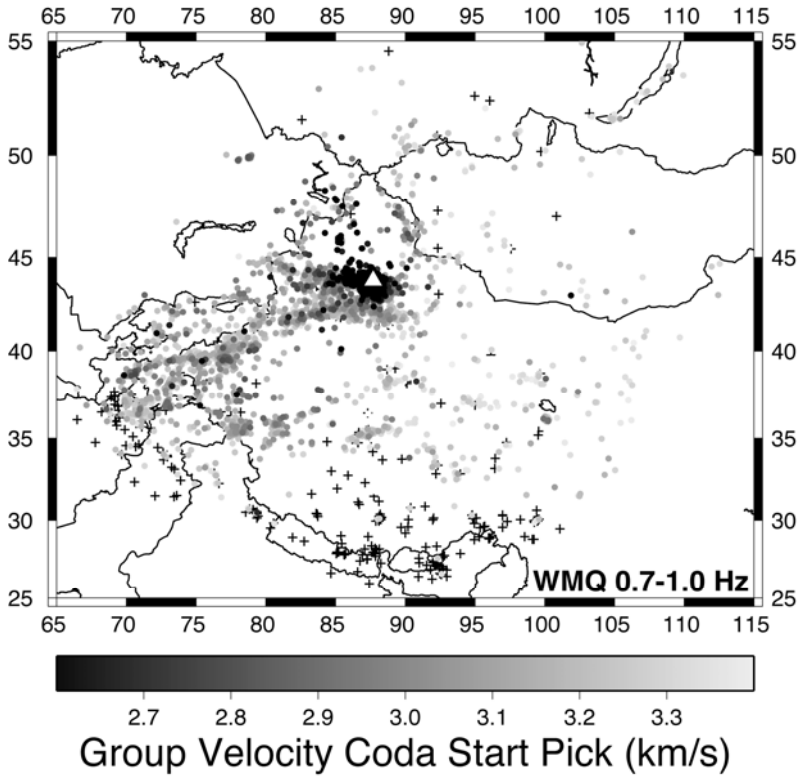

Figure 3. Geographical distribution of the group velocity of the beginning of the coda for station WMQ, band 0.7–1.0 Hz. Group velocities between 2.6 and 3.4 km/s are represented by the gray scale. Group velocities greater than 3.4 km/s are indicated by crosses. The low velocities near the station are due to the standard distance effect. Additional low velocities for events under the Junggar Basin and at the western end of the Tarim basin are 2-D effects. Group velocities are generally slower from western and faster from eastern azimuths.

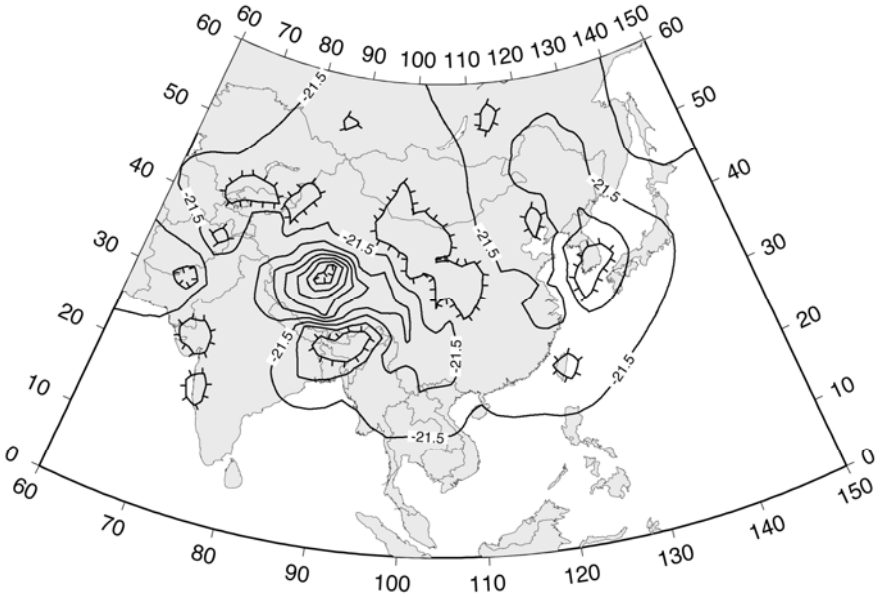

Figure 4. Transfer function (log10 N-s) obtained using a 2-D EGF technique. Contour intervals are 0.1 N-s; the –21.5 N-s contour is annotated. Contour ticks point in downhill directions.

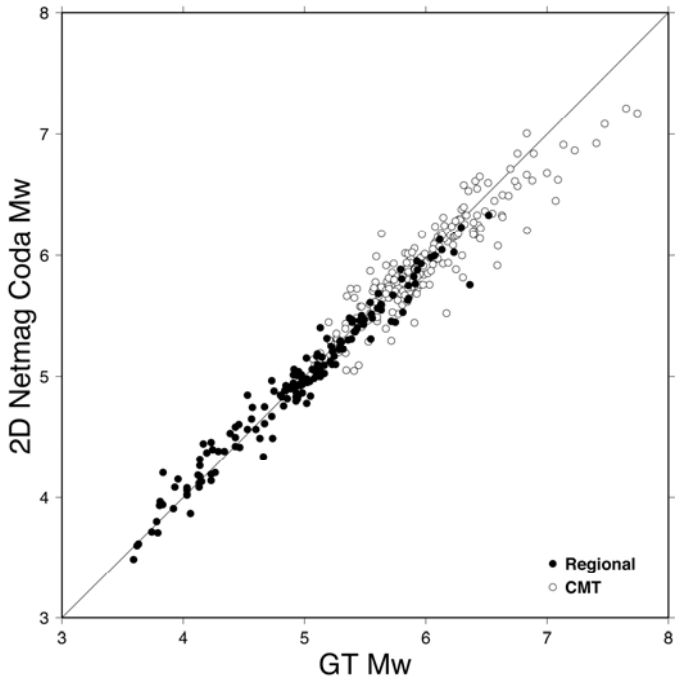

Figure 5. Ground truth (GT) versus coda network Mw. Closed circles indicate regionally derived ground truth Mw for continental events. Open circles indicate Harvard centroid moment tensor (CMT) Mw for oceanic events.

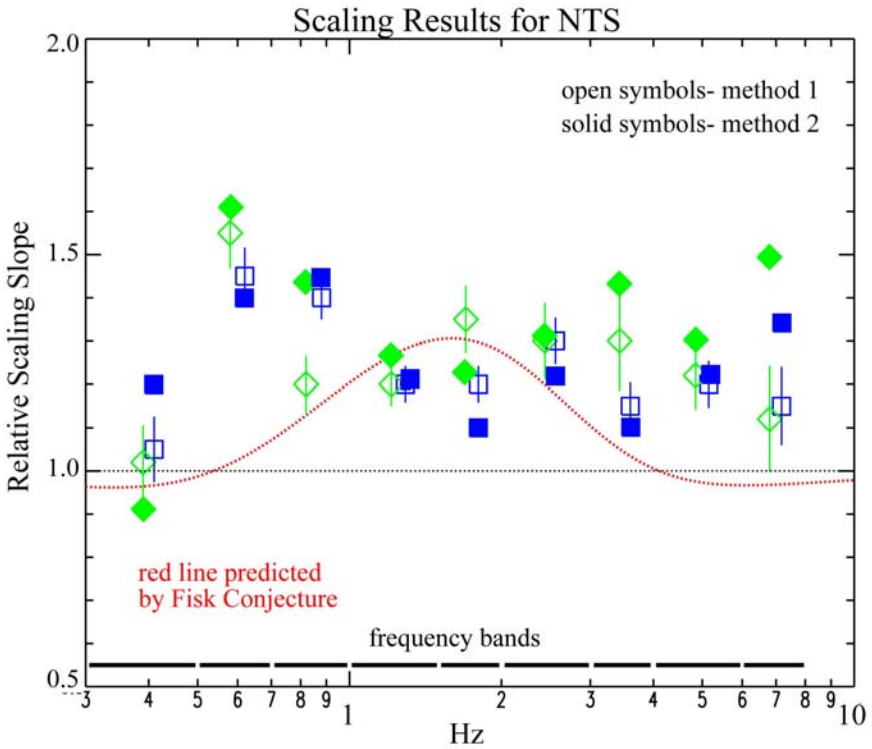

Figure 6. Relative yield scaling slope of Pn with respect to Lg coda waves for NTS explosions. Open symbols with error bars (two sigma on relative slope estimate) are results for method 1, while solid symbols are results for method 2 obtained by taking the ratio of the slopes from yield regressions, Pn/LgCoda. For example, the results of the 0.5–0.7 frequency band show that Pn slope is ~1.5 times larger than the slope for Lg coda waves. The red dotted line is a prediction of the relative scaling slopes based on the Fisk conjecture and the Mueller and Murphy explosion source model.

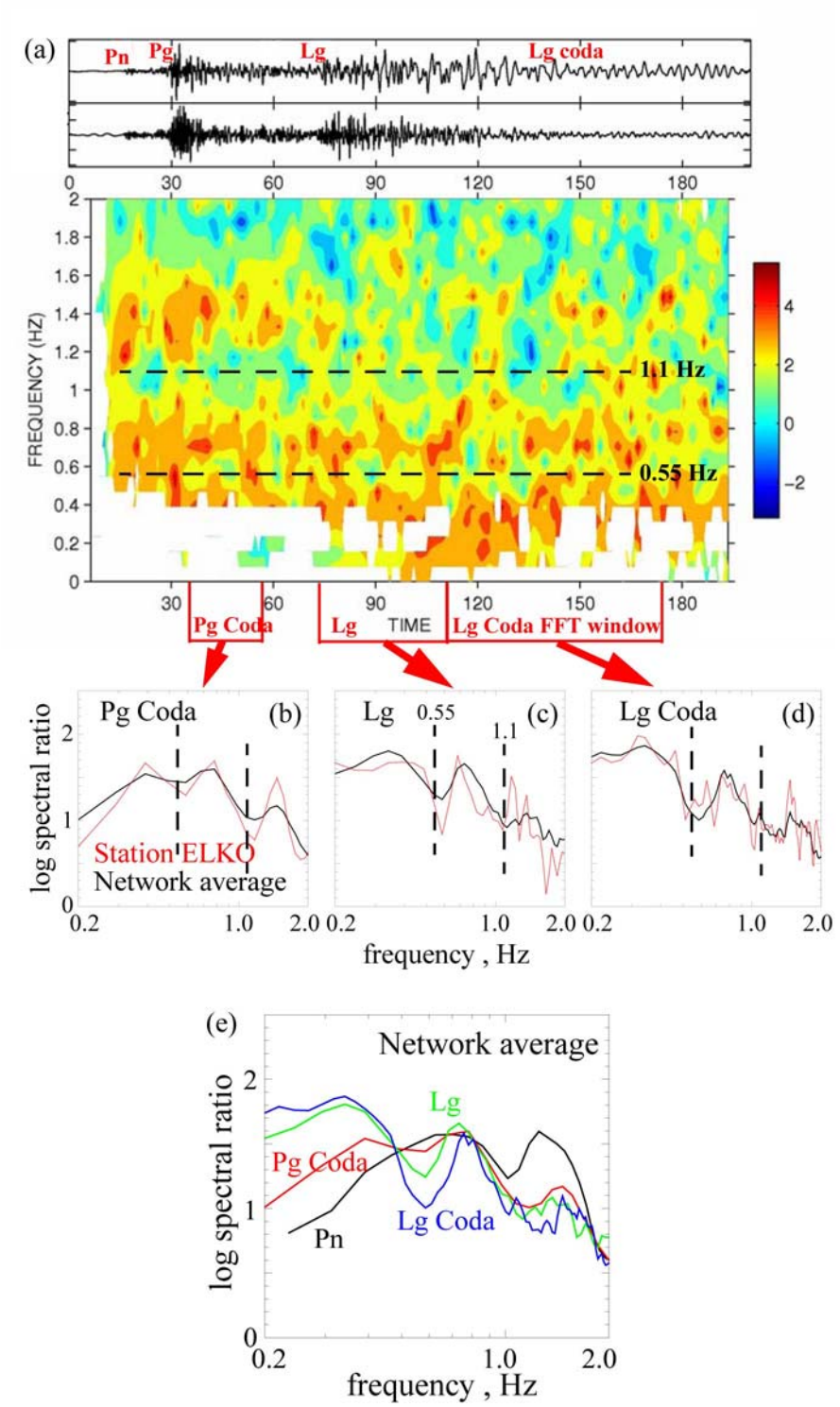

Figure 7. (a) Rousanne-Techado difference spectrogram for ELK (seismograms plotted at the top). Dash lines are positioned over nulls at 0.55 and 1.1 Hz. The null at 0.55 Hz is observed in Pg coda, Sn, Lg, and Lg coda. The null at 1.1 Hz is also observed in the Pn phase. (b)–(d) Spectral ratios for the time windows shown on the abscissa of the spectrogram plot corresponding to Pg coda, Lg, and Lg coda. (e) Summary of the spectral ratios for Pn, Pg coda, Lg, and Lg coda. Signal-to-noise ratio is marginal below 0.3–0.4 Hz.